STRUCTURAL CONTROL AND HEALTH MONITORING
Struct. Control Health Monit. 2008; **15**:622–641
Published online 17 July 2007 in Wiley InterScience
(www.interscience.wiley.com) DOI: 10.1002/stc.219

Reliability of dynamic identification techniques connected to structural monitoring of monumental buildings

Stefano Podestà[1], Giuseppe Riotto[1,*,†] and Francesco Marazzi[2]

[1] *Department of Civil, Environmental and Architectural Engineering, University of Genova, Genova, Italy*
[2] *Freelance, Brinzio (Va), Varese, Italy*

SUMMARY

The impossibility of adjusting the monumental buildings to the protection levels adopted for newly conceived buildings brings about the need to accept lower safety levels. In such case, the potentiality of dynamic monitoring by means of periodic checks on the dynamic characteristics of the structure (its own frequencies and vibration modes) would allow, at least theoretically, one to check globally that there are no changes to the boundary conditions that would further diminish the structural safety level. To this end, the dynamic analyses of a masonry triumphal arch of a medium-sized church are reported in this paper. The dynamic identification campaign was carried out at the ELSA Laboratory, studying the in-plane behaviour of the structure in undamaged and damaged conditions. The dynamic identification campaign, which lasted more than 6 months, allowed us to test the reliability of different acquisition systems, of different typologies of excitation and above all of evaluating the influence of environmental conditions on the dynamic parameters that may be identified. Indeed, variation of the environmental factors (e.g. temperature, insolation, humidity) may determine a change of the structure's own frequencies that must be taken into consideration just so as to be able to recognize the variations that may be correlated to a structural change due to the presence of damage. Copyright © 2007 John Wiley & Sons, Ltd.

KEY WORDS: structural health monitoring; monumental masonry buildings; dynamic identification reliability; damage detection; boundary conditions

1. INTRODUCTION

Structural health monitoring (SHM) was traditionally considered as observing the evolving behaviour of a structure over time. This original meaning is now being progressively enriched: in order to evaluate the structural behaviour of a church, a bridge or a tower, it is very important not to limit at the mere recording of the physical variables involved in the ageing process (crack

*Correspondence to: Giuseppe Riotto, Department of Civil, Environmental and Architectural Engineering, University of Genova, Via Montallegro 1-16145, Genova, Italy.
† E-mail: riotto@diseg.unige.it

Received 6 November 2006
Revised 3 May 2007
Accepted 15 May 2007

opening or closing, inclination, base settlement, temperature, etc.), but also to interpret these data. The real target of a monitoring testing campaign is, in fact, the judgement of the building safety, regarding the recognized evolutionary pattern of the measured quantities. Accordingly with advanced international research in this field, this latter meaning is what we intend by SHM [1].

The technique is based on consolidated technologies of dynamic characterization and identification of structures: the knowledge of the modal parameters allows the choice of a variable set that can be considered as the structure's fingerprint. The monitoring of these variable set permits us to observe the fingerprint's evolution: any change of the initial condition has to be interpreted as a mutated structural condition that can be related, eventually, to a reduced safety level.

A further step is usually to localize the damage along the structure [2]. This topic can be very significant for bridges, for example, where this information can be used to target the retrofitting intervention. For monumental historical buildings, damage localization can be very hard to perform due to their extreme complexity and hyperstatic behaviour, but the burdensome traditional visual inspections would be reduced for the results of a SHM that assure the presence of damage. In a building, the damage mechanism control, with the proposed methodology, can ensure, in fact, a proper safety level greater than what can be obtained with traditional methodologies. In this sense the definition of 'structural intervention' can be enlarged to a methodology that allows the safety monitoring of a structure over time. The comparison between the initial behaviour of the building with the actual one provides a kind of structural data very hard to obtain with traditional static loading tests [3].

The research is based on the dynamic characterization of a masonry triumphal arch built at the ELSA Laboratory specifically for SHM analyses. Starting from the study of the undamaged arch, the changing response of the structure due to an induced damage was considered.

Some studies [4, 5] have shown that the variability in the natural frequency values due to changed ambient conditions can be of the same order of magnitude as structural damage modification effects. In this case, the intrinsic variability hides the damage modification on structural parameter response, making damage assessment *via* dynamic identification impossible. This prompted the authors to perform a complete preliminary analysis to evaluate the range of structural dynamic parameters for the original configuration. After this preliminary phase, structural damage was induced in the arch through a prearranged settlement of a foundation.

A proper comparison and analysis between the initial chosen variable set and the corresponding ones at each damage induced step will give an index of the overall damage that occurred.

2. THE STRUCTURAL MODEL

Accordingly with the goal of using dynamic identification processes for SHM of monumental structures, a proper structural model was built. The constructed arch has the same scale and the same materials as a real structure and was erected with the same construction technique. The choice of the arch typology as representative of historical structures was suggested by the fact that this structural typology is almost always present inside historical monumental churches. Even if built with different architectonical styles, the churches (80% of the monumental heritage in Italy), are characterized by a recurrent typology where it is possible to recognize different structural elements (macroelements). The triumphal arch is almost always present as the

DOI: 10.1002/stc

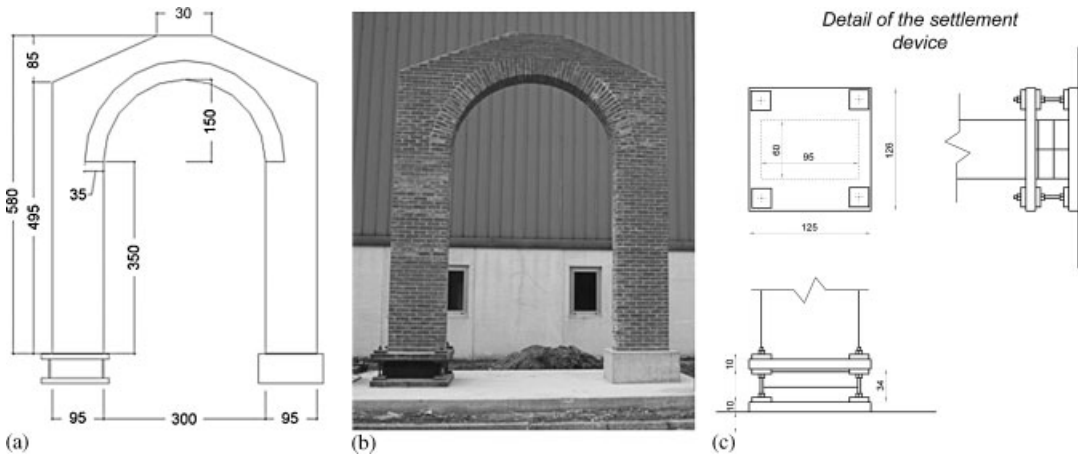

Figure 1. The arch: (a) dimensions; (b) front view; and (c) settlement device detail.

separation element between the church hall and the presbyteral–apse zone. In churches with only one nave (a very frequent typology), it is constituted by a masonry wall with a wide arch opening. This macroelement is characterized by in-plane seismic response in spite of its slight stiffness out of plane; the presence of the church hall and of the presbytery and/or apse prevents, in fact, the activation of an out-of-plane collapse mechanism [6].

A preliminary study to the model was performed in order to individuate a triumphal arch representative of a small–medium size church. To this aim, we have analysed the geometrical data of more than 3000 churches surveyed after the 1997 Umbria-Marches earthquake in Italy.

The testing arch was constructed outside the ELSA Laboratory in order to take into account the climatic variations similar to those observed in ordinary real buildings (Figure 1).

The goal of studying the modification of the dynamic parameters after a structural damage had spurred the authors to design a proper lowering mechanism to be placed under one of the columns in order to simulate the effects of a base settlement. The prototype was built, therefore, with one column on a concrete block while the other on a steel mechanical device that can be regulated in height as shown in Figure 1.

To properly choose the kind of instrumentation to be used for the dynamic identification and for the following monitoring phases, a preliminary numerical simulation of the arch response was carried out with a FEM model (ANSYS code).

The arch was modelled with respect to both the geometry and its mechanical parameters ($E = 2000$ MPa; $G = 750$ MPa; $\rho = 1800\,\mathrm{kg/m^3}$). The first three natural frequencies and mode shapes of the in-plane behaviour are reported in Figure 2.

The 'blind test' achievement permitted the evaluation of the arch natural frequencies and mode shapes, in order to individuate the best position of the accelerometer sensors with respect to the region with zero displacement and to the expected crack pattern after the base settlement [7].

The result was an accelerometer wire made up of 15 accelerometer sensors with horizontal measurement axes and one accelerometer sensor with vertical measurement axes; finally, a more precise accelerometer sensor was placed on the West side of the arch with variable measurement axes (it was possible to change its direction accordingly with the aims of the specific test, Figure 3).

DOI: 10.1002/stc

Figure 2. First three in-plane natural frequencies and mode shapes obtained from FEM analysis: 7.02, 22.15 and 35.79 Hz.

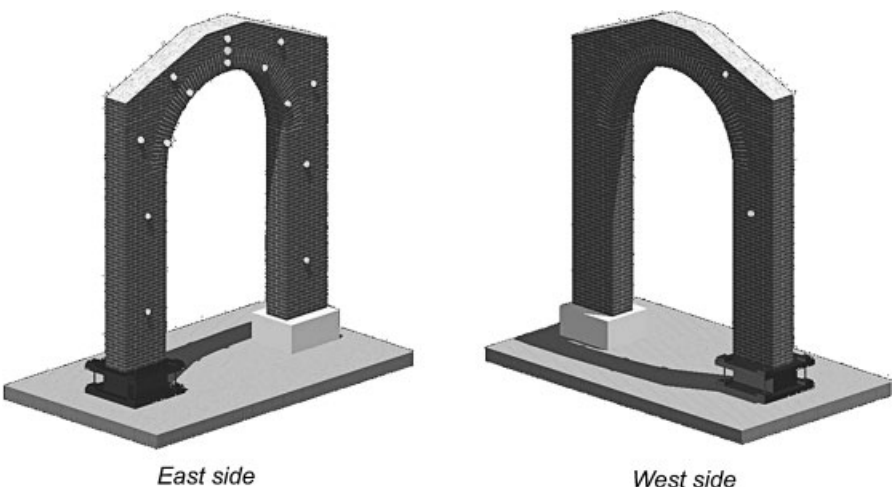

Figure 3. Schematic view of the sensor placement: East side and West side.

Although the research is focused on the identification of in-plane response, it was necessary to evaluate the out-of-plane dynamic response of the model, analysing the response of two accelerometer sensors, appositely positioned on the West façade. The results of the out-of-plane testing campaign are not reported in this paper for reasons of brevity [8].

3. THE TESTING CAMPAIGN

The testing campaign was conducted, from April to September 2004, at the ELSA Laboratory of the Joint Research Centre of the European Commission and at the Department of Civil, Environmental and Architectural Engineering of the University of Genoa.

The tests were performed with the instrumented hammer (*PCB 086C50*) equipped with a soft head in order to excite the lower frequencies and mode shapes of the arch.

DOI: 10.1002/stc

The impact of the hammer was always induced in plane on the columns nearly 3.30 m above ground level. The signals coming from the load cell of the hammer and from the accelerometer sensors were recorded with an acquisition sampling time of 200 Hz using a low-pass filter with cutting frequency at 80 Hz, in order to minimize the aliasing effects. The high damping of the hammer suggested the reducing of the time length of the recorded signals to 20 s with starting time 0.05 s before the hit (this was possible because of properly set pre-trigger values on the acquisition recorder). The corresponding frequency definition is thus 0.05 Hz. An exponential window with a decay constant of 4 s was also applied to the recorded signals in order to reduce the distortion due to instrumental noise [9].

From the analysis of the recorded signals, the *frequency response function* (*FRF*) was computed [10] (Figure 4). The results clearly shown that, in plane, two resonance frequencies at 8.65 and 46.05 Hz can be located on the FRF plot *via* the *peak picking* method. In the central part of the FRF plot, a double peak at nearly 28 Hz can be found (27.40 and 28.30 Hz).

Analysing the complete test series, however, it was possible to recognize the real cause of this double peak due to the presence of an out-of-plane natural frequency very close to the in-plane second natural frequency. The analysis of the recorded accelerometer sensor signal with horizontal measurement axes out of plane, clearly, shows the resonant peak at 27.40 Hz (Figure 5(a)).

A further confirmation was deduced by analysing the FRF of the accelerometer with vertical measurement axes (Figure 5(b)). This direction is excited mainly by the second in-plane natural mode shape, as it can be assumed from the modal shape obtained *via* numerical analysis (Figure 2). The modal shapes corresponding to each measured natural frequency were reconstructed using the imaginary part of the FRF of the installed accelerometer sensors. It is worth remembering that all the sensors have horizontal measurement axes, while the structural deformation also has a vertical component: in any case the observed mode shapes are completely similar to those obtained with the 'blind' numerical preliminary model (Figure 6).

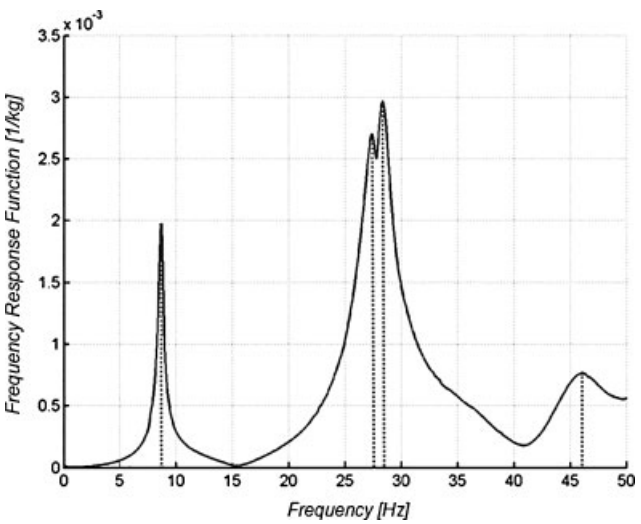

Figure 4. FRF of one accelerometer sensor.

DOI: 10.1002/stc

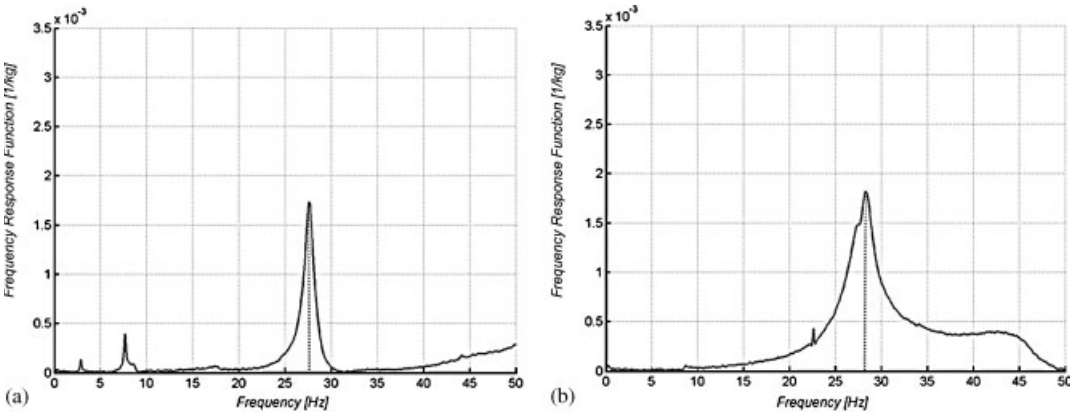

Figure 5. FRF along different directions: (a) FRF along the out-of-plane horizontal axis and (b) FRF along the vertical axis.

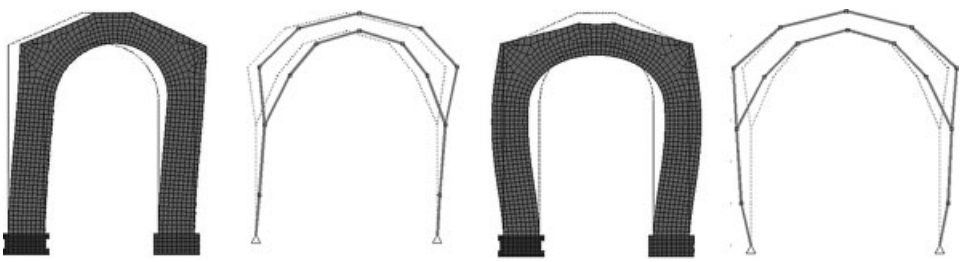

Figure 6. I and II natural in-plane mode shape: numerical and experimental results.

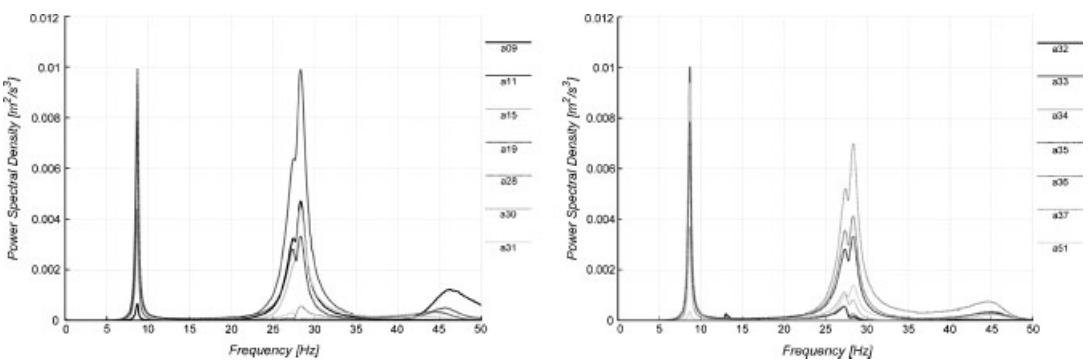

Figure 7. PSD of the all the accelerometers on the west side.

In order to simulate an 'output only' analysis, the hammer signal was not considered and the power spectral density (PSD) function of each recorded signal was calculated (Figure 7). The natural frequencies were the same as those obtained *via* the FRF analysis.

DOI: 10.1002/stc

The advantages of an 'output only' analysis are relevant with respect to the more classical FRF analysis in order to develop a methodology that can be easily applied to real structures. In this case, the number of registration channels and the acquisition system performance needed can be reduced, thereby lowering the costs. Moreover, the SHM, on a real structure, has the considerable advantage of not having the hammer connected to the acquisition system, thus permitting easier and faster movements.

4. RESULTS VARIABILITY

The testing campaign consisted of 36 tests conducted on the triumphal arch before inducing any damage (undamaged structure—*Step0*) using the instrumented hammer as forcing. The repetition of some tests in apparently the same conditions has shown that a certain amount of variation, in terms of the natural frequencies of vibration, was present. This scattering has to, obviously, be attributed to factors that are independent of structural damage and represents a 'physiological' aspect of the proposed SHM method [11]. In order to properly evaluate the reliability of the proposed method, the different boundary conditions were analysed in detail. It is relevant to understand their origin and, surely more important, to quantify their entity [4]. The analysis was performed on the first and second in-plane natural frequency, while the third in-plane natural mode shape was not considered because its scattering was too high even inside a single test (see Figure 7).

The sources of variability investigated were:

- intensity of the impact due to the instrumented hammer;
- impact location;
- ambient conditions.

This analysis was then repeated for each level of induced damage in order to identify the variation range of the natural frequencies due to these phenomena in the different structural states.

4.1. Impact intensity

The frequency variation due to the impact intensity was observed from the first tests carried out. It was noticed that tests conducted very close in time during the same day (so with the same weather conditions, temperature, etc.) presented different results in terms of frequency. The first hypothesis was connected to the variation given by the non-linearity of the structure. To check this hypothesis, some tests were carried out with the following scheme: five hits were given with *normal* intensity (no more than 800 N) and five hits with *high* intensity (no less than 1200 N), calculating, in the end, the mean of the two classes. Analysing the test results, obtained considering the more precise accelerometer sensor (*Kinemetrics EpiSensor FBA ES-U*), with *normal* intensity (test: a117) and with *high* intensity (test: f117), the following PSD can be obtained (Figure 8).

In particular, if the amplitude of the PSD near the resonance frequency is compared, it is easy to notice that there is a frequency variation between the two kind of hit. Especially in the second natural frequency, a clear reducing in the frequency peak value, due to the increasing in the hammer hit force, is clearly visible. The observed variations can only be caused by the different

DOI: 10.1002/stc

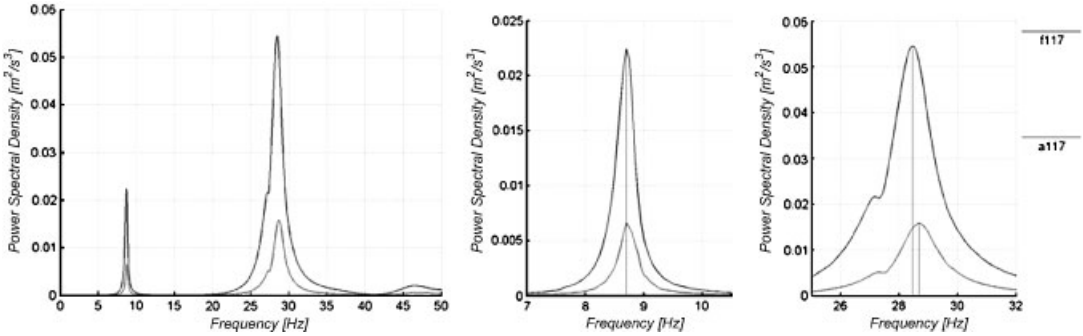

Figure 8. PSD of the test a117 and f117: I and II natural frequencies.

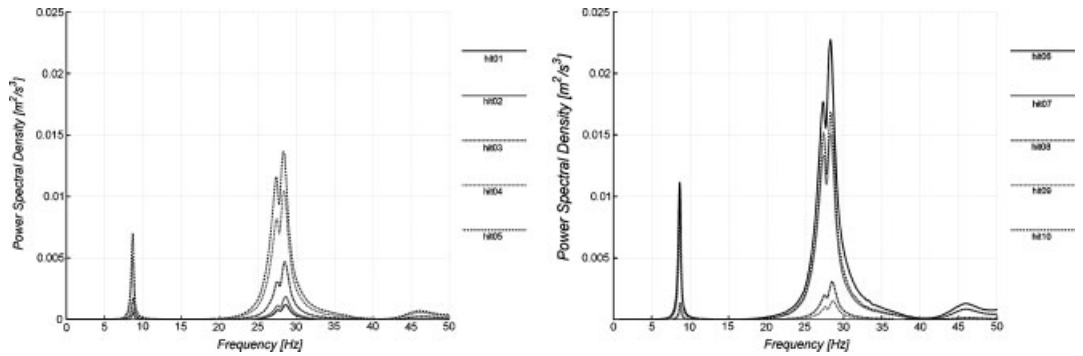

Figure 9. PSD of a test series: I and II natural frequencies.

hammer impact intensities because they were obtained hitting at the same location and in similar ambient conditions, (consecutive tests). Analogous results can be obtained for all the signals coming from the accelerometer sensors placed on the structure for all the other tests. In order to evaluate the influence of the hit intensity on the natural frequencies more precisely, a set of tests with forcing hit of different intensities were also performed. The pattern of these tests was: five consecutive hits with *normal* intensity (no more than 800 N) and the other five with variable intensity. The very short period of test execution (15 min) permits us to consider the ambient conditions constant inside the same series of data. The obtained PSD of the analysed signals of the 10 hits of each test series are shown in Figure 9.

By plotting the peak value of the PSD with respect to the frequency relative to the I and II natural mode shapes, it is possible to determine the decreasing frequency value with respect to the increasing amplitude of the PSD (Figure 10): this effect is more evident on the II natural frequency of vibration.

The peak value of the PSD of the acceleration signal was considered representative of the area limited by the PSD curve near the peak itself. This area is proportional to the energy related to that specific natural mode shape, so the PSD peak value became a direct measure of how much energy excited that particular resonance frequency. In case the hit is not completely on the symmetry axes of the structure (e.g. if it is not exactly in the middle plane of the arch), the peak

DOI: 10.1002/stc

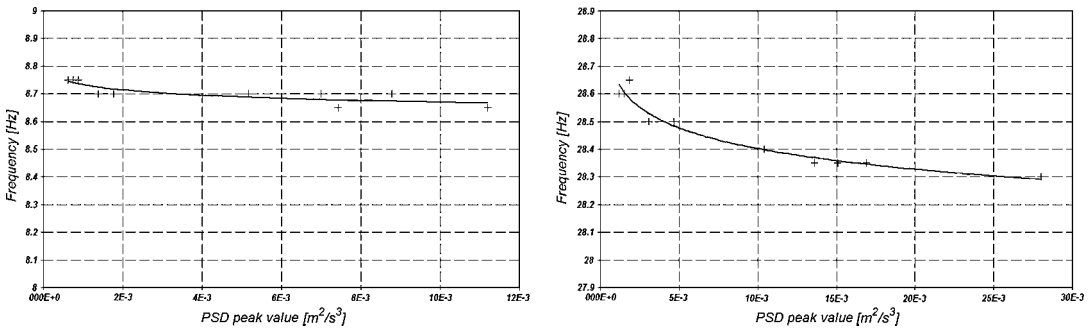

Figure 10. Natural frequencies *vs* PSD peak amplitude: different hit intensities.

PSD value still gives useful information about the excitation of the structural in-plane natural mode shapes. This information is more reliable than the value of the forcing hit that cannot take into account the case of non-perfect hits.

The maximum range of the scattering frequencies due to the different intensities of the hits for all the performed series of tests is 0.15 Hz for the I natural frequency and 0.85 Hz for the II natural frequency (respectively around 1.7 and 3% of the medium value of the natural frequencies). A possible reason of this variation could be connected to the non-linear stiffness of the structure.

4.2. Impact location

The location of the impact point is another important parameter to be taken into account because it can considerably influence the dynamic response of the structure [12]. In order to evaluate the variability range connected with impact location, some dedicated tests were performed on the arch, hitting the structure at different locations but taking care to impose an almost constant intensity (at a nominal value of 800 N). The hit series was obtained striking the columns at six different locations with heights varying from ground level to 3.30 m (hit 01–06: left column; hit 07–12: right column).

The variations obtained, as in the previously described case with different hit intensities, cannot be due to different ambient conditions because, also in this case, the execution time of one hitting series is lower than 15 min.

Observing the natural frequencies *vs* the PSD peak value (Figure 11) it is easy to notice the frequency variation related to the I and the II mode due to the different forcing locations. Also in this case their frequency tends to decrease when the PSD peak increases.

This behaviour is completely similar to that previously stated for the variation due to the different impact force hits. If the PSD peak increases the corresponding resonance frequency decreases. To hit the structure at different locations, if ambient conditions are not changed and if the hit is given with roughly the same force, determines necessarily different oscillation amplitudes, so inducing the same non-linear responses observed in the previously described case.

Taking into account the maximum range of the scattering frequencies due to the impact locations for all the performed series of tests, the obtained variability is 0.25 Hz for the I natural frequency and 0.60 Hz for the II natural frequency (respectively around 2.9 and 2.1%).

DOI: 10.1002/stc

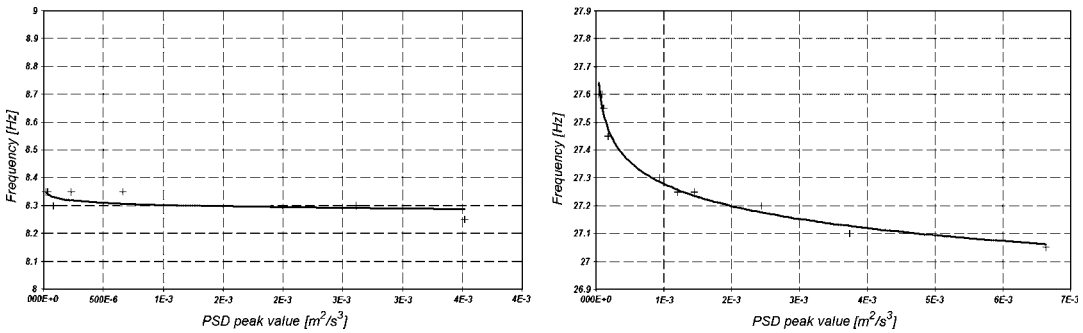

Figure 11. Natural frequencies *vs* PSD peak amplitude: different hit locations.

Table I. Temperature and natural frequencies.

Ambient temperature (°C)	I frequency (Hz)	II frequency (Hz)
20.1	8.35	27.25
23.7	8.65	28.35
26.2	8.85	28.70
27.7	8.90	28.55
27.9	8.80	28.20
26.2	8.65	27.75

4.3. Ambient conditions

The influence of the natural frequency variation with respect to the ambient conditions was analysed after the evaluation of the variability range due to the location and hit intensity. The study of this parameter was evaluated considering the data obtained striking the arch on the left columns at 3.30 height from ground level with *normal* hits (no more than 800 N). In this way, we tried to minimize the influence of the previously described source of variation. The maximum difference between the natural frequencies is 0.60 Hz (6.9%) and 1.90 Hz (6.7%) for the I and the II natural frequency, respectively. In order to explain this high variability, a testing campaign was performed for an entire day, in such a way to have different temperatures for each test. The temperatures and frequency values resulting from the analysis are reported in Table I.

Normalizing these three series of data (the two frequencies and the temperature) with respect to the maximum value recorded for each of them during the day, the following graph can be drawn (Figure 12).

It can be noticed that the vibration frequencies initially grow during the day until a maximum value, then decrease at sunset and this variation is directly correlated to the natural progress of the temperature. The maximum values of the temperature and of the frequencies, however, do not take place at the same time. This behaviour is probably related to the fact that more sophisticated correlation models must be considered between these two variables, for example, the real temperature of the structure should also be taken into account. Plotting the two frequencies *vs* the recorded ambient temperature (for the only tests performed with a *normal* hit on the same location) it is possible to see a general tendency to increase of the frequencies with the temperature values (Figure 13), but a clear correlation function is hard to obtain.

DOI: 10.1002/stc

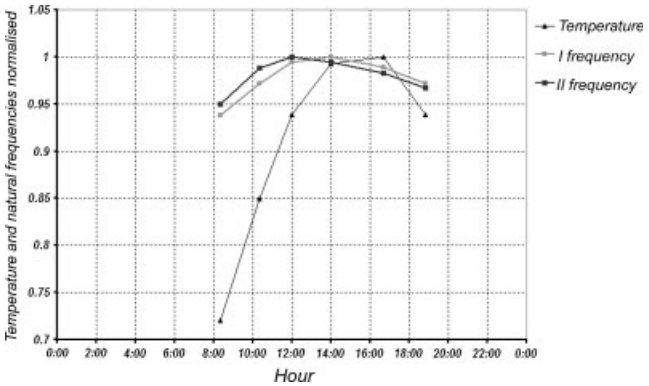

Figure 12. Temperature and frequencies normalized compared to the maximum value.

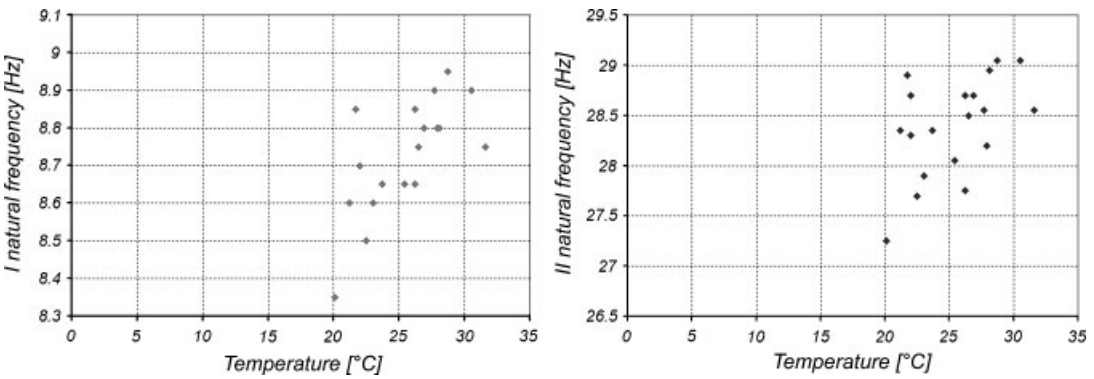

Figure 13. Temperature *vs* I and II natural frequencies.

Another parameter that could influence the variability of a dynamical identification is the water absorbed by the structure. Bricks are very porous material and a significant amount of water absorbed can lead to a not negligible increase in structural masses. In this case, the water absorbed by the bricks is due to the fact that the arch was subject to intense rain for several days. Even if a deep inspection of this phenomenon was not possible for test timing reasons, we noticed that the peak values of the 'wet' arch were slightly lower than those obtained with under 'dry' conditions, confirming the hypothesis (Figure 14).

The natural frequencies recorded during all the tests have been summarized. The variability due to the different impact forces is shown for each test reporting the maximum and the minimum frequency value obtained by the analysis of that test. Inside this value range, the typical value (i.e. the value obtained calculating the mean of the tests performed with *normal* force) is marked. These values obtained for each test are then placed side by side on the same graph in order to evaluate the variability due also to the ambient condition and the impact position. The results are reported in Figure 15 for the first and the second natural frequency, respectively.

DOI: 10.1002/stc

Figure 14. Wet arch due to rain.

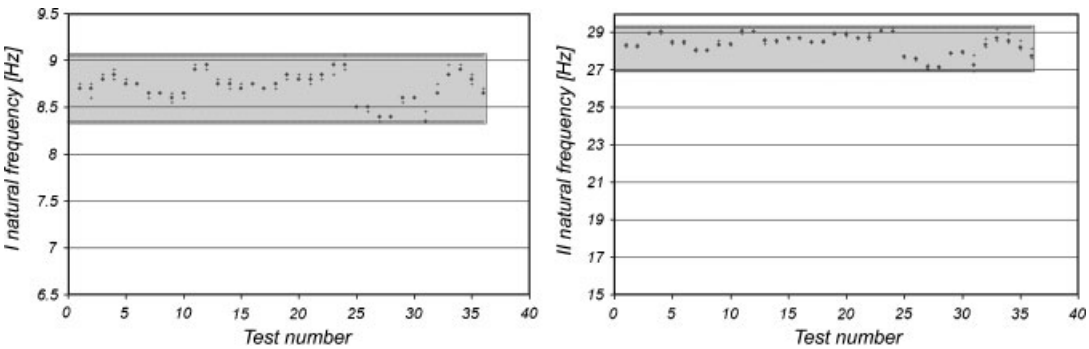

Figure 15. Variability of the I and II natural frequencies for all the tests performed.

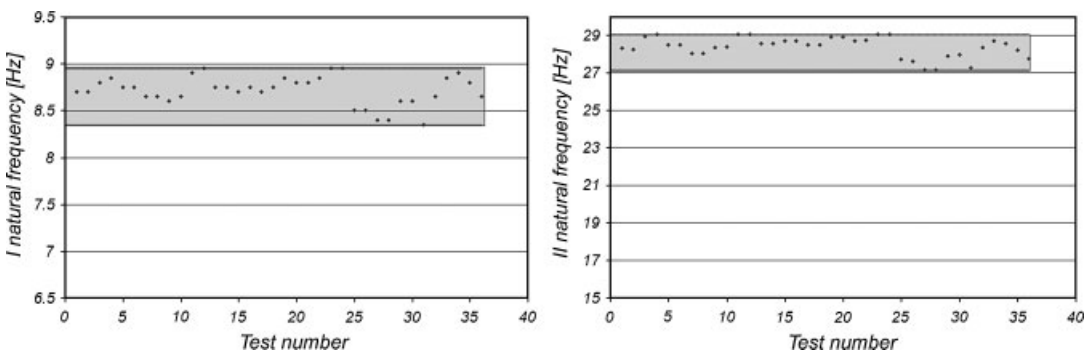

Figure 16. Variability of the I and II natural frequencies for the all normal impact tests.

DOI: 10.1002/stc

The scattering of the measured natural frequencies obtained during the testing campaign can be considerably reduced eliminating those causes of variation that can be easily controlled during the tests. Thus considering only the tests obtained with *normal* impacts at a height of 3.30 m from ground level on the column with steel bearing, the graphs in Figure 16 can be obtained.

From all the sources of frequency variability, the ambient conditions were recognized as the most important; we have treated the ambient conditions as an uncertainty source and any test as a single occurrence of a stochastic process. The final results of the identification are therefore a frequency range instead of a single value.

The extreme values (maximum and minimum) of this test set are shown with two continuous lines. It must be noticed that these values do not represent a statistical confidential interval, but in any case, they can be useful to assess the frequency range of the undamaged structure, providing an idea of the frequency scattering that can be expected by variable ambient conditions during the test campaign.

5. DAMAGE DETECTION

After the dynamic identification on the undamaged structure (*Step0*), a limited damage was induced through a low settlement (i.e. 5 mm on the left column). A provisional structure was

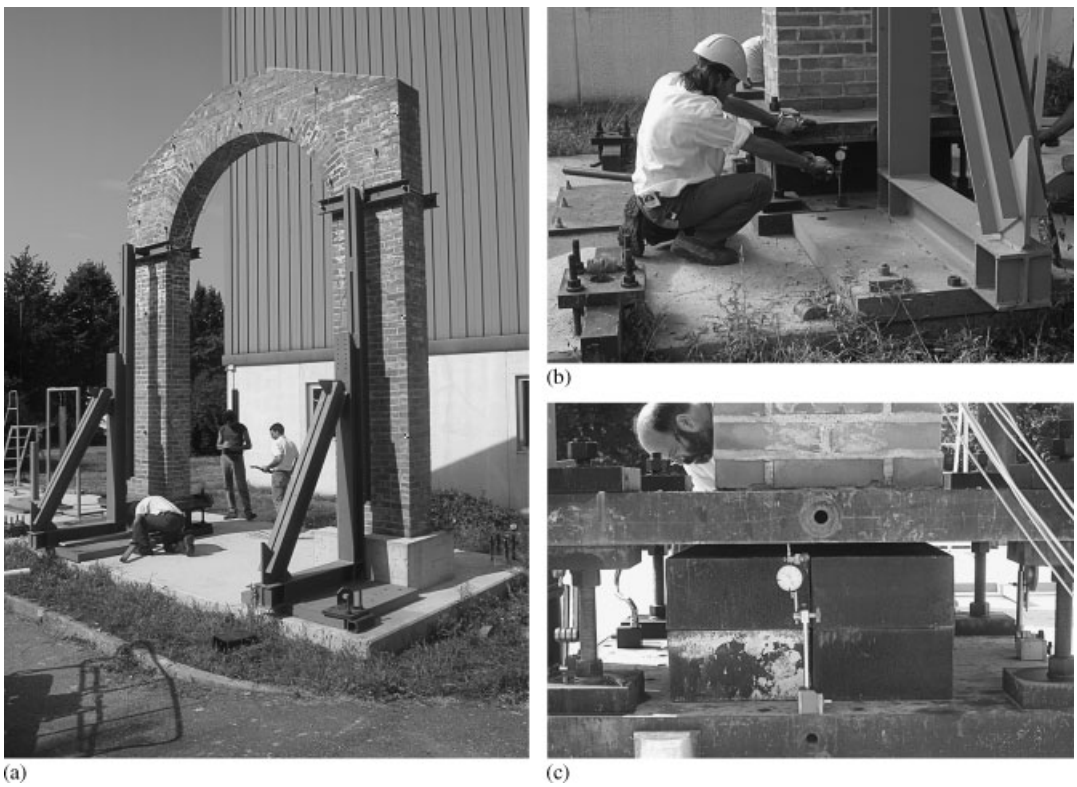

Figure 17. Settlement: (a) provisional structure and (b) and (c) lowering operations.

DOI: 10.1002/stc

placed in the vicinity of the arch (but not in contact with it) in order to permit safe operations without changing the dynamic properties of the test structure (Figure 17(a–c)).

Tests were performed with the instrumented hammer already used during *Step0* (undamaged structure).

As for the undamaged structure, the test repetition (18 tests) showed a frequency variation. The FRF and the PSD of the acceleration signal of the test with frequency content closer to the mean of the recorded values during the testing campaign are reported in Figure 18.

The comparison with the analyses performed for the undamaged structure reveals that the double peak at the second in-plane frequency completely disappeared in this new damage configuration (*Step1*).

As shown in Table II, damage induces modifications mainly to the in-plane modes, while the out-of-plane modes are very slightly influenced. It is also important to notice that damage modifies the order of presentation of the natural modes; in particular, it exchanges the IV and V modes [8].

Besides the frequency identification, the natural mode shapes were also determined. The comparison between the two in-plane natural mode shapes shows an almost complete

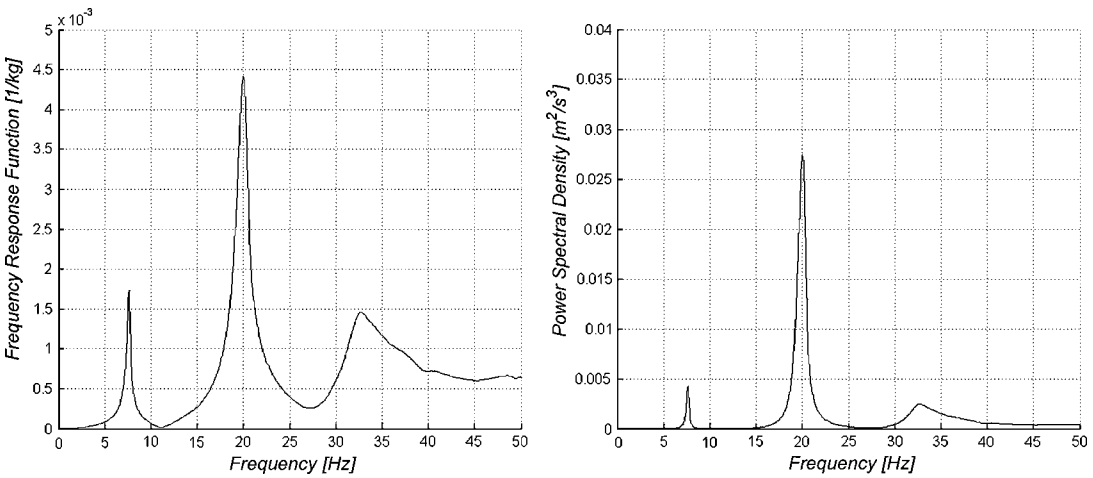

Figure 18. FRF and the PSD of the acceleration signal.

Table II. Comparison of natural frequencies in *Step0* and *Step1*.

	Undamaged structure (*Step0*)		Damaged structure (*Step1*)	
Mode	In plane (Hz)	Out of plane (Hz)	In plane (Hz)	Out of plane (Hz)
I	—	2.70	—	2.60
II	—	7.40	—	6.60
III	8.65	—	7.65	—
IV	—	16.85	—	14.80
V	—	27.40	20.00	—
VI	28.30	—	—	23.55

DOI: 10.1002/stc

indifference to damage, i.e. the two vibration modes are practically identical, even if the associated vibration frequency was subjected to an important reduction (Figure 19).

The damage level is, in fact, minimal (the maximum crack amplitude is in the order of 1 mm). Moreover, the crack pattern is localized at the arch intrados, avoiding the activation of local vibration natural mode shapes (Figure 20) [11, 12].

A comparison between the PSD curves of two representative tests, one for *Step0* (undamaged structure) and the other for *Step1* (5 mm settlement) clearly shows that the natural frequencies have lowered as a consequence of the inserted damage in the arch (Figure 21).

Analogously to the previously described testing campaign (*Step0*), the appraisal of the influence of ambient temperature and force excitation on the recorded frequencies was performed.

In Table III, the temperatures measured and frequency values resulting from the tests are reported.

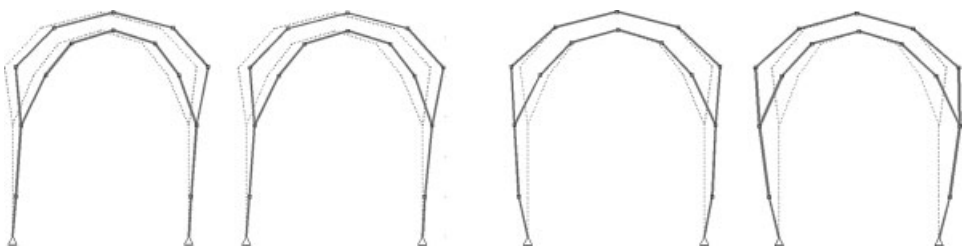

Figure 19. Comparison of natural mode shapes in *Step0* and *Step1*.

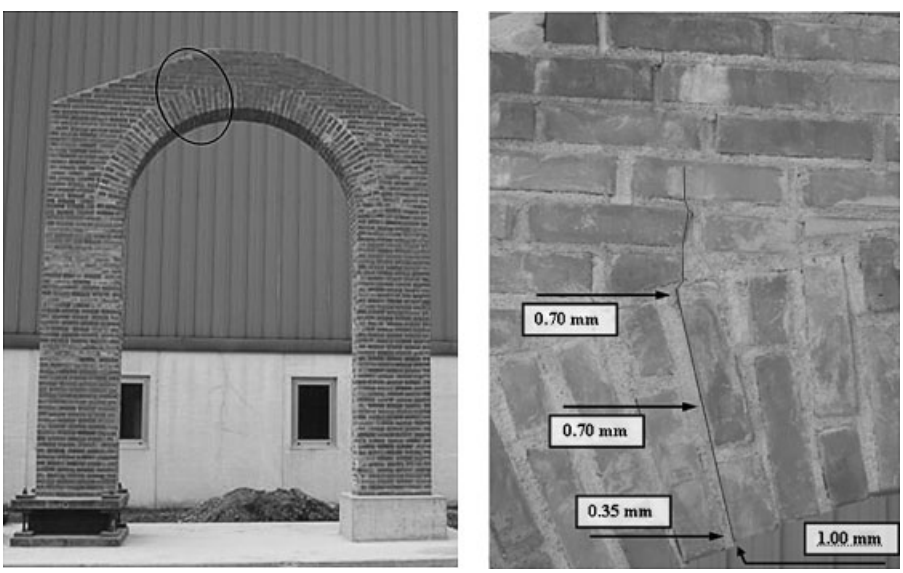

Figure 20. Position and amplitude of crack pattern.

DOI: 10.1002/stc

Normalizing these three series of data (the two frequencies and the temperature) with respect to the maximum value recorded for each of them during the day, the following graph can be drawn (Figure 22).

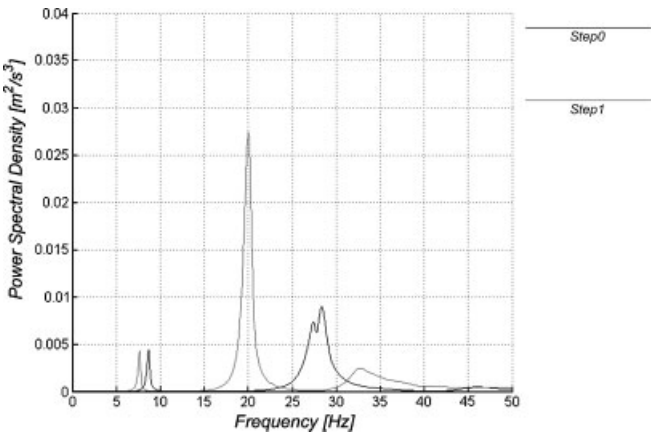

Figure 21. Comparison of in-plane PSD for *Step0* and *Step1*.

Table III. Temperature and natural frequencies.

Ambient temperature (°C)	I frequency (Hz)	II frequency (Hz)
20.4	7.70	20.85
21.5	7.70	20.70
23.8	7.85	21.00
28.0	8.00	21.25
26.3	7.85	20.85
23.7	7.75	20.45

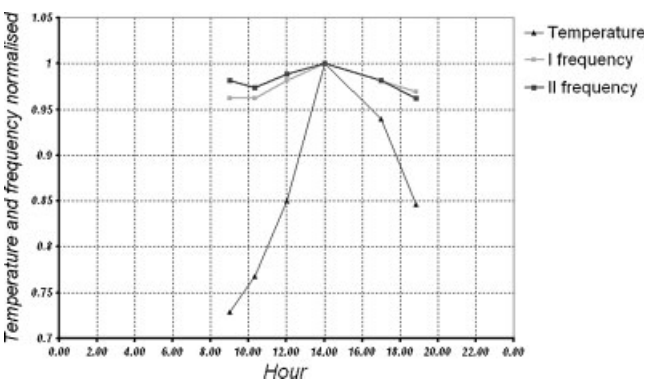

Figure 22. Temperature and frequencies normalized compared to the maximum value.

DOI: 10.1002/stc

It is worth observing a similar correlation between the natural frequencies and the temperature values as that individuated for the undamaged condition (Figure 12). But, in this case, the maximum values are simultaneous.

As already shown for the undamaged condition (Figure 13), by plotting the obtained two frequencies *vs* the recorded ambient temperature (for the only tests performed with a *normal* hit on the same location) it is possible to notice a general tendency to increase for the frequencies when the temperature increases (Figure 23).

Also, the results variability due to hit intensity variation is analogous to *Step0* (Figure 14). By plotting the peak value of the PSD with respect to the frequency relative to the I and II natural mode shapes, it is possible to determine the decreasing frequency value with respect to the increasing amplitude of the PSD (Figure 24).

Figure 25 summarizes all the natural frequencies related to the first and the second in-plane modes as were obtained during all the tests executed in *Step0* and *Step1*. The frequency variation due to the different intensity in hitting the structure is also reported for each single test.

As already shown for *Step0* the scattering of the measured natural frequencies can be reduced eliminating the dependencies from the impact location and intensity. The results are shown in

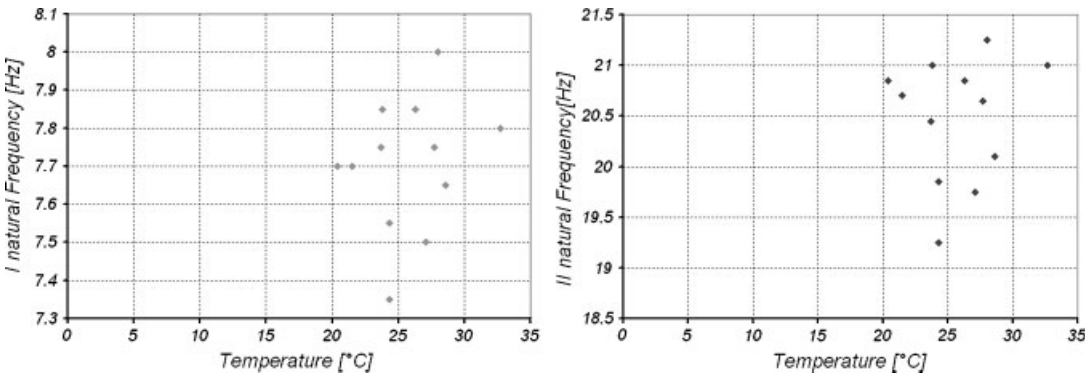

Figure 23. Temperature *vs* I and II natural frequencies.

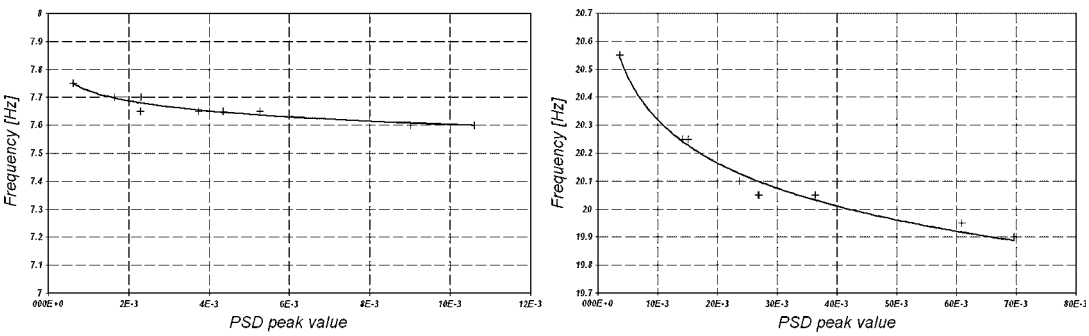

Figure 24. Natural frequencies *vs* PSD peak amplitude.

DOI: 10.1002/stc

Figure 26. The frequency variation range for *Step0* and *Step1* tests can be grouped into two well-separated set. The groups are, in fact, sufficiently narrow to permit their separation: the variation in the first natural frequency due to damage insertion is higher than the variation due to different ambient conditions or testing force intensities, although the light damage level caused by the base settlement. In a dynamic monitoring, this aspect allows the individuation of the damage, in sense of the possibility to associate the frequency variation to a structural change. For a complex structure (i.e. monumental building) dynamic characteristic variation (known the physiological part due to the ambient condition) could permits, rather than a precise damage localization, the activation of alarm thresholds useful to plan a more accurate inspection (traditional visual survey).

The analysis of the second natural frequency shows a similar behaviour (Figure 26). Also in this case the two sets of frequencies are well separated, thus allowing damage detection *via* frequency shift observation.

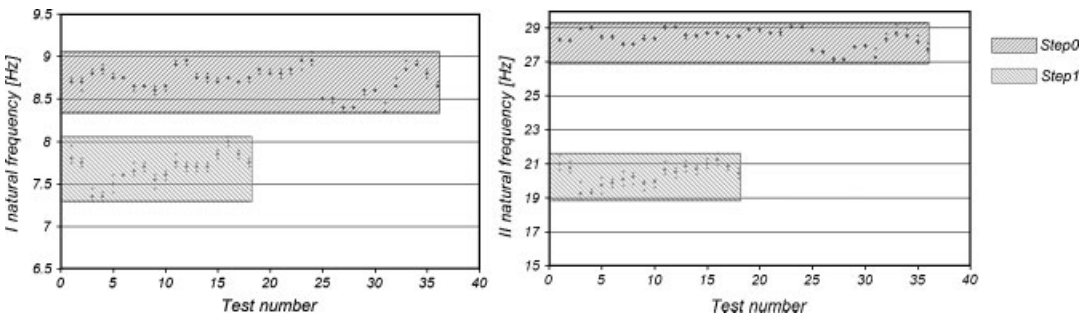

Figure 25. Variability of the I and II natural frequencies for all the tests in *Step0* and *Step1*.

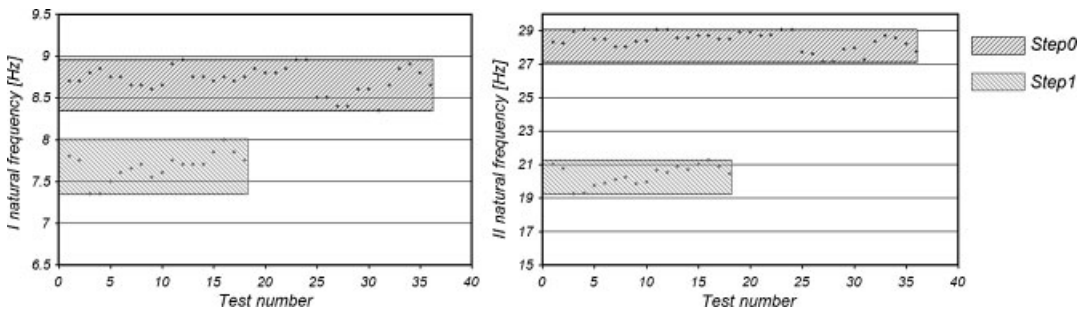

Figure 26. I and II natural frequencies range for all normal hit tests in *Step0* and *Step1*.

Table IV. Comparison of natural frequency range in *Step0* and *Step1*.

	I natural frequency range (Hz)	Scattering (Hz)	Medium percentage	II natural frequency range (Hz)	Scattering (Hz)	Medium percentage
Step0	8.35–8.95	0.60	6.9	27.15–29.05	1.90	6.7
Step1	7.35–8.00	0.65	8.5	19.25–21.25	2.00	9.8

DOI: 10.1002/stc

In Table IV, the frequency range for the first and the second natural frequencies is shown for both the previously described steps.

The frequency scattering due to the ambient conditions is nearly the same (in percentage) inside any single *Step*. From *Step0* to *Step1*, it is possible to notice an increase that could be probably related to the temperature influence on the crack opening. On the other hand, the shift in the mean value of the I and II frequencies is very clear: even if the inserted damage was of little importance, the vibration properties of the arch allows revelation of the crack presence.

6. CONCLUSIONS

The results, presented in the paper, show that the natural frequencies obtained from the test campaign of a prototype of triumphal arch are highly dependent on the boundary conditions and in the way the tests are performed. This aspect may be negligible for a common dynamical identification, but it is crucial for SHM based on the periodical control of natural frequencies. It is important to know whether the observed variation in these parameters can be attributed to an evolving damage or simply to different testing conditions: the reliability of a dynamic monitoring of a real structure is subordinate, first of all, to a precise individuation of the frequency variation aliquot not affected by ambient condition change. From this point of view, several set of tests were performed hitting the structure with an instrumented hammer in the undamaged and damage conditions (*Step0* and *Step1*).

The analysis of the results has evidenced a clear dependence of some parameters from the hit intensity and position and from the ambient conditions (e.g. temperature, wetting, etc.). For each of these parameters, with different levels of reliability, the variation interval was obtained. These values have to be taken into account when a periodical check of the dynamic characteristics of the structure is performed in order to monitor the safety level of a real structure. This aim is, normally, relevant for the cultural heritage, for which the need to preserve its historical and architectonical value prevents the adjusting of the safety level to the one fixed for the new conceived buildings. To accept a lower safety level is only possible whether the building is periodical under control, in order to guarantee the minima requirement. From this point of view, the dynamic monitoring could be interpreted as one of the retrofitting techniques, able to solve the dichotomy between conservation and safety of historical masonry buildings.

ACKNOWLEDGEMENTS

The Authors thank Prof. Sergio Lagomarsino and Prof. Georges E. Magonette, who supported this research.

REFERENCES

1. Johnson EA, Beck JL, Faravelli L, Mita A. Future directions for structural health monitoring. In *Proceedings of the 4th International Workshop on Structural Control*, New York, U.S.A., 10–11 June 2004, Smyth A, Betti R (eds). DEStech Publications: New York, U.S.A., 2004; 177–181.
2. Faravelli L, Farina M, Marazzi F. Genetic algorithms for structural identification. In *Proceedings of the 9th International Conference on Structural Safety and Reliability* (*ICOSSAR2005*), Rome, Italy, 19–23 June 2005, Augusti G, Schuëller GI, Ciampoli M (eds). Millpress: Rotterdam, Netherlands, 2005; 3115–3121.

DOI: 10.1002/stc

3. Calderini C, Lagomarsino S, Podestà S, Resemini S. Historical engineering and structures in Italy. Part II: Structural behaviour diagnosis and monitoring. *Proceedings of the I Convegno Nazionale di Storia dell'Ingegneria*, Naples, Italy, 8–9 March 2006. Cuzzolin Editore: Naples, Italy, 2006; 659–669 (in Italian).
4. Peeters B, De Roeck G. One year monitoring of the Z24 bridge: environmental influences versus damage events. *Proceedings of the 18th International Modal Analysis Conference* (*IMAC-XXVIII*), San Antonio, TX, 7–10 February 2000; 1570–1576.
5. Feltrin G. Environmental effects on eigenfrequencies of a RC highway bridge. In *Intelligent Structures*: *An Overview on the Ongoing European Research*, Baratta A, Corbi O (eds). Consorzio Editoriale Fridericiana: Naples, Italy, 2003; 61–73. ISBN: 88-8338-025-8.
6. Lagomarsino S, Podestà S, Resemini S, Curti E, Parodi S. Mechanical models for seismic vulnerability assessment of churches. In *Structural Analysis of Historical Constructions*, Modena C, Lourenço PB, Roca P (eds), vol. 2; *Proceedings of the IV International Seminar SAHC* (SAHC'04), Padua, Italy, 10–13 November 2004. A.A. Balkema: London, U.K., 2004; 1091–1101.
7. Renda V, Magonette G, Molina J, Tirelli D, Marazzi F. Activities of the European Laboratory in the field of structural control for civil buildings, bridges and architectural heritage. In *Proceedings of the 3rd International Workshop on Structural Control*, Casciati F, Magonette G (eds), Paris, France, 6–8 July 2000. World Scientific: London, U.K., 2000; 463–472.
8. Damonte G, Riotto G. Dynamic monitoring for monumental buildings conservation: experimental result on a masonry arch. *Degree Dissertation*, Department of Structural and Geotechnical Engineering, University of Genoa, Genoa, Italy, 2005 (in Italian).
9. McConnell KG. *Vibration Testing*. *Theory and Practice*. Wiley: New York, U.S.A., 1995.
10. MATLAB. The Math Works Inc. MA, U.S.A., 1997.
11. Beni F, Lagomarsino S, Marazzi F, Magonette G, Podestà S. Structural monitoring through dynamic identification. In *Proceedings of the Third World Conference on Structural Control*, Casciati F (ed.), vol. 3, Como, Italy, April 2002. Wiley: West Sussex, U.K., 2002; 139–146.
12. Marazzi F, Podestà S, Magonette G, Lagomarsino S, Beni F. Structural health monitoring of monumental building. In *Proceedings of the First European Workshop on Structural Health Monitoring*, Balageas DL (ed.), Paris, France, 10–12 July 2002. CD-ROM, paper number 9.

DOI: 10.1002/stc